

# Fabrication and properties of 2D EBGs by moulding/demoulding with high permittivity ceramics

Jianzhang Shi · Hong Wang · Tingwei Yao · Feng Xiang · Xi Yao

Published online: 21 August 2007  
© Springer Science + Business Media, LLC 2007

**Abstract** Two-dimensional electromagnetic bandgap structures (2D EBGs) are designed and fabricated by moulding/demoulding. A high permittivity and low dielectric loss microwave material,  $\text{Bi}_2\text{O}_3\text{-ZnO-Nb}_2\text{O}_5$  (BZN) was used. The impacts of high permittivity on the 2D EBGs' properties are investigated. As the experiments showed, wide electromagnetic band gap is found in the frequency ranges from 5.6 to 10.6 GHz, and 12.6 to 16.6 GHz. The first gap is greater than 60% of the gap center frequency, while the second gap is 25% of the center frequency. The interval between the two gaps is larger than 2 GHz, and the return loss of both gaps is as large as  $-40$  dB. This interesting phenomenon of multi band gaps is very useful for diplexers, multi-mode tunable dielectric antennas and resonators. Based on these, expansive applications may be exploited in the future. The experimental results are in good agreement with the simulations'.

**Keywords** Two dimensional electromagnetic band gap structure (2D EBGs) · Multi band gaps · Moulding/demoulding · High permittivity ceramics

## 1 Introduction

Electromagnetic bandgap structures (EBGs) are periodic dielectric or metallic materials, which can exhibit wide band pass and band rejection properties at certain microwave frequencies. Since the concept was introduced in 1987 [1, 2], EBGs have become one of the most interesting areas of research. Inasmuch as only 3D EBGs are ideal to manipulate the transmission properties of wave at will, most of the efforts have been aimed to them. Various trials have been conducted, and a great lot of fabrication technologies for 3D EBGs have been reported until recently, such as layer by layer method [3, 4], angle etching [5], colloidal precipitation [6, 7], photopolymerization method [8, 9], and so on. And 3D arrangement of elements and wiring have been adopted in electronic devices to formulate highly integrated components, thus it is expected that future photonic devices will also adopt 3D structure. However, although 3D EBGs are essential for the realization of photoelectric integrated circuits, 2D EBGs have received increasing attention because they can be easily obtained using conventional semiconductor processing. Even with the weakness of imperfect band gaps, 2D EBGs have surprisingly revealed their usefulness in many domains, for instance, waveguides [10], resonators [11], antennas [12], fibers [13], lasers [14], etc.

However, present existing technologies for fabricating EBGs appear to have several shortcomings in the lack of flexibility in both design and materials. For example, angle etching method requires a very high accuracy, thus the severe etching conditions tend to weaken the high symmetry of the structure. The colloidal precipitation faces the difficulties to fabricate large scale ordered structures or introduce controlled defects in the structure. The layer by layer method, by frequently dry etching, polishing, and

---

J. Shi · H. Wang (✉) · T. Yao · F. Xiang · X. Yao  
EMRL, Key Laboratory of Ministry of Education,  
Xi'an Jiaotong University,  
Xi'an 710049, China  
e-mail: hwang@mail.xjtu.edu.cn

J. Shi  
School of Technical Physics, Xidian University,  
Xi'an 710071, China



**Fig. 1** A honeycomb sample of 2D EBGs by moulding/demoulding

heating, encounters difficulties in multilayer and introduction of various materials and defects. Otherwise than these mentioned above, the materials used for EBGs are mainly with focus on the semiconductors and other low permittivity materials—Si, SiO<sub>2</sub>, InP, GaAs, metal, etc., and the techniques are often involved in semiconductors processing. So far appropriate techniques and detailed discussions for high permittivity ceramic 2D EBGs have not been reported.

Here we proposed a novel fabrication method for ceramic 2D EBGs by the concept of moulding/demoulding, and a honeycomb 2D EBGs sample was designed and fabricated with material of Bi<sub>2</sub>O<sub>3</sub>-ZnO-Nb<sub>2</sub>O<sub>5</sub> (BZN), which has high dielectric constant and low dielectric loss at microwave frequency. And the impacts of high permit-

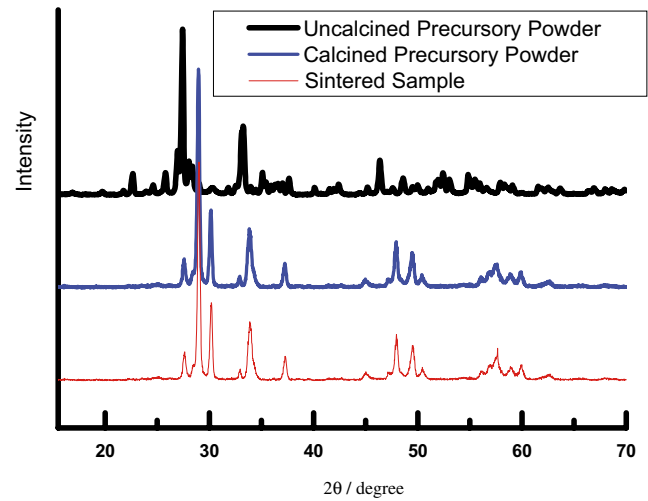


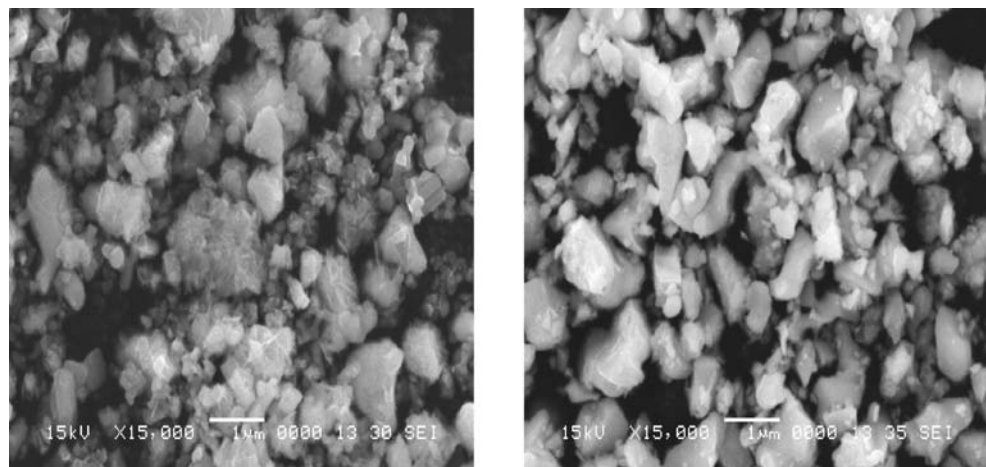
**Fig. 3** XRD of precursory powders and EBGs sample

tivity on the 2D EBGs’ properties are investigated in detail. Compared with other fabrication technologies it has several evident advantages. First of all, the procedure is simpler, easily to obtain accurate symmetric structures. Next, the controlled defects are easy to be introduced, with less damage to 2D EBGs. Finally, this method is suitable for the application of a mass of ceramic materials. In brief, this technique provides great potential for the fabrication of 2D EBGs within the frequency range of microwave and millimeter wave.

## 2 Sample preparation

First, chemical reagent Bi<sub>2</sub>O<sub>3</sub>, ZnO and Nb<sub>2</sub>O<sub>5</sub> as starting materials were weighed according to the composition

**Fig. 2** SEM photographs of precursory powders. (a) Uncalcined powder, (b) calcined powder



(a)

(b)

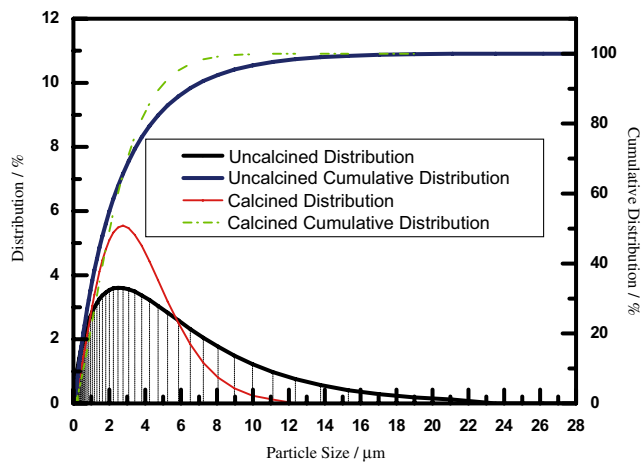


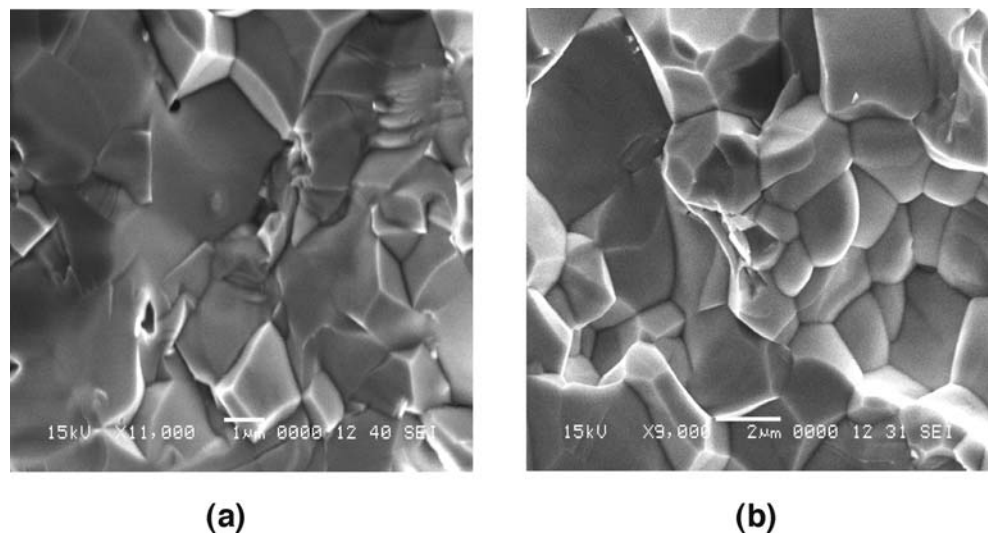
**Fig. 4** Particle size distribution

$3\text{Bi}_2\text{O}_3:2\text{ZnO}:3\text{Nb}_2\text{O}_5(\text{BZN})$ . After twice ball milling and drying, the powder was calcined at  $800\text{ }^\circ\text{C}$  for 3 h. Then ball milling and drying again, granule manufacture was performed carefully, waiting for mould injection.

At the same time, the melting wax was pulled into a die, and then cooled down to the room temperature under the pressure of 40 MPa. After that, a well shaped wax mould was obtained by etching a designed EBGs pattern on it.

Subsequently, the wax mould was steadily put into the die again. Once the precursory powder was injected into the wax mould, a pressure of 30 MPa was applied on it. After five or ten minutes, the wax mould with the solidified ceramic body was taken out from the die. Then the wax mould was removed from the green ceramic body by heating up to about  $160\text{ }^\circ\text{C}$  in an oven. Finally, the primary sample was sintered in the furnace at the temperature of  $960\text{ }^\circ\text{C}$  for 4 h. Up to this point, a precision 2D EBGs was

**Fig. 5** Cross section of 2D EBGs sample. (a) With uncalcined powder, (b) with calcined powder



obtained. One picture of 2D honeycomb EBGs sample is shown in Fig. 1.

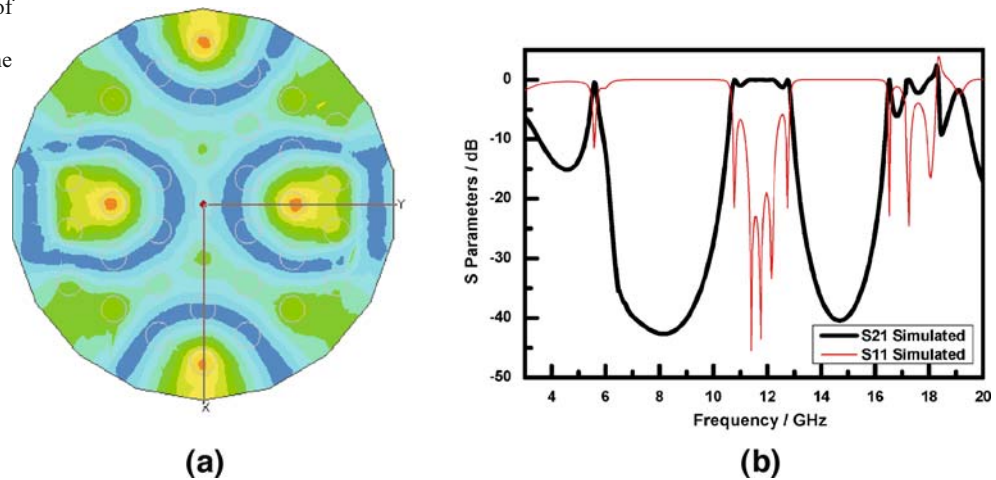
With the view of evaluating the effects of precursory powders on the final sample of 2D EBGs, several types of examinations have been made, including the grading analysis by the WQL-11 Granularity Analyzer, the crystallographic form analysis by DC1000 XRD Analyzer, and the surface and cross section analysis by SEM JSM-6360LV.

The SEM photographs of calcined and uncalcined precursory powders are shown as Fig. 2(a) and (b). With the aim of distinguishing the difference of process technique, the XRD analysis was also carried out, as shown in Fig. 3. From these photos, we can see obviously that granularity of calcined precursory powders was slightly larger than that of uncalcined, but the particle size is more homogeneous. The curves of granular distributions, shown in Fig. 4, are in accord with these. And the crystallographic form of calcined powder is much closer to the final sample, which results in much less shrinkages during the sintering procedure, thus avoiding a great many of microfractures or other damages to the 2D EBGs sample. The more homogeneous distribution of calcined precursory powders will also increase the fluidity during the moulding, thus help the moulding and compactness of our EBGs samples. These results can be validated from the cross section pictures of sintered EBGs. As Fig. 5 shows, the cross section of EBGs rod with the calcined powder is more uniform than that of uncalcined and the grains are more compact with less defects and microcracks. The high accuracy of microstructures is sufficient for the practical use.

### 3 Numeric simulation and measurement

In order to further illustrate the characteristics of moulding/demoulding technology and the impacts of high dielectric

**Fig. 6** The simulation results of 2D EBGs. (a) The distribution diagram of electric field. (b) The transmission and reflection coefficients



constant ceramic on the 2D EBGs properties, numeric simulation and experimental measurement were also conducted.

According to the designed pattern of 2D honeycomb EBGs fabricated by moulding/demoulding (shown in Fig. 5), the parameters of simulation model were picked up, with high permittivity material of BZN,  $\epsilon_r=76$ ; and the low dielectric materials of polymethyl methacrylate (PMMA),  $\epsilon_r=2.2$ . And the radius of rods was 1 mm and the lattice constant was 4 mm. For the purposes of simplifying the simulation, the dielectric materials were considered perfect, i.e. the dielectric loss was zero. The simulation results of transmission characteristic and energy distribution are shown in Fig. 6. The transmission and reflection coefficients (S11 and S21) plots, obtained by the numeric simulation, corresponded to a case of transverse magnetic mode (TM; i.e. electric field parallel to the rods).

As compared to EBGs reported before with the low permittivity materials, an interesting phenomenon—a useful second gap—is observed. In addition, the center of band gaps

shifts to low frequency obviously, and the ratio of bandwidth to the gap center frequency becomes larger, also the band gap becomes deeper. As can be seen from the graphs, a wider electromagnetic band gaps are found in the frequency ranges from 5.6 to 10.8 GHz and 12.6 to 16.6 GHz. The first gap is greater than 60% of the gap center frequency, while the second gap is 25% of the center frequency. The interval between the two gaps is larger than 2 GHz. The return loss of both gaps is as large as  $-40$  dB. Meanwhile, these results are mostly confirmed by the measurement experiments with Vector Network Analyzer 8720ES by and large, as shown in Fig. 7. The main differences between two graphs exist in the shifts of central frequency of band gaps to lower frequency and the sharply ripples in the rejection band. Nevertheless, in consideration of the shrinkage of 2D EBGs dimension caused by sintering and the errors of measurement system, the results of experiments are in good agreement with the simulations'.

#### 4 Conclusions

In this paper, we proposed a novel fabrication method for ceramic 2D EBGs by the concept of moulding/demoulding. A 2D honeycomb EBGs sample was designed and fabricated with material of BZN, which has high permittivity and low dielectric loss at microwave frequency. Compared with other fabrication technologies it reveals several evident advantages. So this technique provides great potential for the fabrication of 2D EBGs within the frequency range of microwave and millimeter wave.

And the impacts of high permittivity on the 2D honeycomb EBGs' properties are investigated in detail, by means of numeric simulation and measurement. As compared to EBGs reported before with the low permittivity materials, an interesting phenomenon—a useful second gap—is observed. In addition, the center of EBG shifts to low

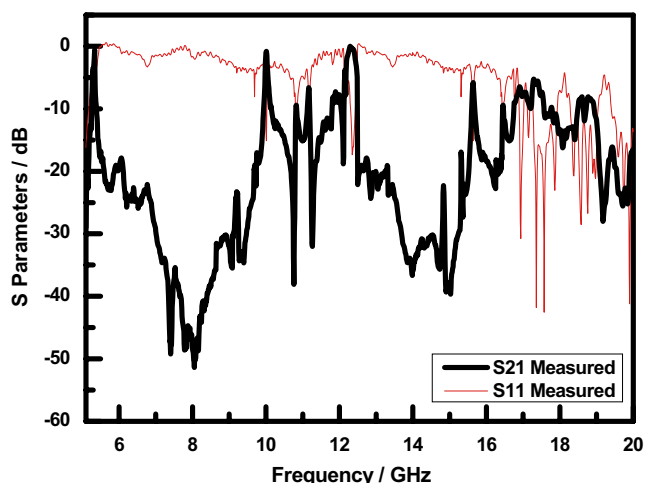


**Fig. 7** The measurement results of 2D EBGs

frequency obviously, and the ratio of bandwidth to the gap center frequency becomes larger, also the band gap becomes deeper. This interesting phenomenon is very useful for diplexers, multi-mode tunable dielectric antennas and resonators. Based on these, expansive applications may be exploited in the future.

**Acknowledgements** This work was supported by NSFC project of China under grant 50572085, National 973-project of China under grant 2002CB613302 and Key Science and Technology Research Project from the Ministry of Education of China (Grant No. 03155).

## References

1. E. Yablonovitch, Inhibited spontaneous emission in solid-state physics and electronics *Phys. Rev. Lett.* **58**, 2059–2062 (1987)
2. S. John, Strong localization of photons in certain disordered dielectric superlattices *Phys. Rev. Lett.* **58**, 2486–2489 (1987)
3. S. Noda, K. Tomoda, N. Yamamoto, A. Chutinan, Full three-dimensional photonic bandgap crystals at near-infrared wavelengths *Science* **289**, 604–606 (2000)
4. J.G. Fleming, S.Y. Lin, I. El-Kady, R. Biswas, K.M. Ho, All-metallic three-dimensional photonic crystals with a large infrared bandgap *Nature* **417**, 52–55 (2002)
5. A. Chelnokov, K. Wang, S. Rowson et al., Near-infrared Yablonovite-like photonic crystals by focused-ion-beam etching of macroporous silicon *Appl. Phys. Lett.* **77**, 2943–2945 (2000)
6. A. Blanco et al., Large-scale synthesis of a silicon photonic crystal with a complete three-dimensional bandgap near 1.5 micrometres *Nature*, **405**, 437–440 (2000)
7. Y.A. Vlasov, X.Z. Bo, J.C. Sturm, D.J. Norris, On-chip natural assembly of silicon photonic bandgap crystals *Nature*, **414**, 289–293 (2001)
8. S. Shoji, S. Kawata, Photofabrication of three-dimensional photonic crystals by multibeam laser interference into a photopolymerization resin *Appl. Phys. Lett.* **76**, 2668–2670 (2000)
9. M. Campbell, D.N. Sharp, M.T. Harrison, R.G. Denning, A.J. Turberfield, Fabrication of photonic crystals for the visible spectrum by holographic lithography *Nature*, **404**, 53–56 (2000)
10. T. Ovidiu, J. Sajeev, Proposed square spiral microfabrication architecture for large three-dimensional photonic band gap crystals *Science* **292**, 1133–1135 (2001)
11. Y. Akahane, T. Asano et al., High-Q photonic nanocavity in a two-dimensional photonic crystal *Nature* **425**, 944–947 (2003)
12. P. de Maagt et al., Electromagnetic bandgap antennas and components for microwave and (sub)millimeter wave applications *IEEE Trans. Antennas Propag.* **51**, 2667–2676 (2003)
13. W.H. Reeves, D.V. Skryabin, Transformation and control of ultrashort pulses in dispersion-engineered photonic crystal fibres *Nature* **424**, 511–515 (2003)
14. S. Noda, M. Yokoyama, M. Imada et al., Polarization mode control of two dimensional photonic crystal laser by unit cell structure design *Science* **293**, 1123–1125 (2001)